4th URSI AT-RASC, Gran Canaria, 19 – 24 May 2024

Split Bregman Image Synthesis in Radio Interferometry

Fernando R. Rannou*(1)(3), Damián Guzmán(1)(3), Miguel Cárcamo(1), Sebastián Pérez(2)(3)
(1) Departamento Ingeniería Informática, Universidad de Santiago de Chile
(2) Departamento de Física, Universidad de Santiago de Chile
(3) Millennium Nucleus on Young Exoplanets and their Moons (YEMS)

Abstract

The Split Bregman (SB) method is a convex optimization algorithm for L1-regularized problems that has been used in denoising, segmentation, reconstruction and other image processing tasks in a compressed sensing setup, but it has received little attention in radio interferometric imaging. It is very efficient and it can be readily implemented in parallel. In this work we apply the SB algorithm and formulate five L1 optimization problems for radio interferometric imaging. We develop an object oriented Python software that facilitates the incorporation a new SB solvers, by inheriting from base classes. We employ two ALMA datasets of protoplanetary disks to test our framework.

1 Introduction

Image synthesis in Radio Interferometry (RI) is a difficult task due to the ill-posed nature of the underlying inverse problem. Image quality is compromised by the several factors including an incomplete and non-uniform sampling measurements, limited integration times, and various noise sources. And despite the fact there are many well-tested reconstruction algorithms in areas other than astronomy that tackle the inversion problem statistically, CLEAN remains the de-facto algorithm used by the community. Perhaps the biggest advantage of CLEAN is that it is a well understood algorithm, and it is always present in reconstruction software in radio astronomy. Since CLEAN is modeled as a collection of point sources and Gaussian functions it produces pleasing looking images. In this sense the resulting model image is quite synthetic if residuals are not added back the model. Other well understood optimization algorithms that have successfully applied to radio astronomy are Maximum Entropy Maximization (MEM) [1, 2] and Regularized Maximum Likelihood (RML) [3]. On one hand, the advantages of these and similar algorithms are that they provide a statistical framework to incorporate prior knowledge based on the data formation process and estimate noise properties accordingly. On the other hand, these algorithms are usually compute intensive, specially if they work directly with observed visibility data, instead of gridded data.

Another class of algorithms that have been applied in many science and engineering applications, including interferometry, are Compressed Sensing (CS) algorithms with ℓ^1 minimization. The theory of CS establishes that a sparse signal can be recovered accurately from significantly fewer measurements than required by the Nyquist sampling frequency as long as: (1) the underlying image is sparse in some transform domain, and (2) the measurement matrix and the sparsity basis matrix are mutually incoherent. Condition (1) is usually satisfied when reconstructing images of protoplanetary disks, which is our target application. These images are usually composed of a centered elliptical emission structure, with or without concentric rings, and spiral arms in a large dark, noisy background. A CS algorithm should be able to reduce these noisy pixels to near-zero magnitude, and thus effectively reducing noise, while preserving image resolution. If the image have large, extended structures filling the field of view, it can be made compressible by sparse coding in an appropriate transform domain. Despite the lacking of the incoherence principle in many imaging applications [6], CS has been successfully applied in radio interferometry [5].

In this work we investigate the performance of the Split Bregman (SB) iteration [4] for image synthesis which is an extension of the Bregman algorithm in CS. As we will show, the algorithm permits the use of multiple convex penalizer terms without compromising reconstruction times. Experiments demonstrate that it is possible to reconstruct high quality images of 2048×2048 pixels, from real data in less than a minute.

2 Split Bregman

SB is a convex optimization algorithm for ℓ^1 regularized problems that decouples the ℓ^1 and ℓ^2 terms reducing the problem to a sequence of unconstrained optimization problems and Bregman updates. For example, in interferometry a simple image synthesis task can be formulated as the following ℓ^1 minimization

$$\min_u ||u||_1 + \mu ||y - RFu||_2^2 \qquad (1)$$

where y is the gridded observed data, u is the intensity image, F is the Fourier transform operator, and R is a subsampling operator. The first term in Equation 1 corresponds to the ℓ^1 penalization that promotes compressibility in the solution, while the second term is the data error term.

SB transforms the optimization problem into a sequence of the following two optimization steps:

$$\text{Step 1} \quad u^{k+1} = \min_u \mu||y - RFu||_2^2 + \lambda||d^k - u - b^k||_2^2 \quad (2)$$

$$\text{Step 2} \quad \begin{cases} d^{k+1} & = \min_d |d|_1 + \lambda||d - u^{k+1} - b^k||_2^2 \\ b^{k+1} & = b^k + (u^{k+1} - d^{k+1}) \end{cases} \quad (3)$$

where d y b are new variables introduced by the SB iteration. Step 1 corresponds to the minimization of a differentiable convex function and in many cases it can be solved efficiently. Step 2 is the minimization of an ℓ^1 regularizer and can also be minimized efficiently with a shrinkage operator, such as soft-thresholding.

The advantage of SB iteration over the original Bregman approach is that former allows the incorporation of multiple regularization terms. For instance, if the signal is compressible in the Wavelet domain, one can formulate the following optimization problem:

$$\min_u |u|_1 + |Wu|_1 + \mu||y - RFu||_2^2 \quad (4)$$

It can be shown that step 1 for this problem reduces to

$$u^{k+1} = F^{-1}K^{-1}F\left(\mu F^{-1}R^T y + \lambda(d^k - b^k) + \gamma W^T(w^k - b_w^k)\right) \quad (5)$$

where $K = (\mu R^T R + (\lambda + \gamma)I)$ is a diagonal matrix, and λ and γ are penalty parameters introduced in the derivation of the algorithm. Inspection of Equation 5 reveals that it can be computed by simple matrix multiplication with diagonal matrices, and Fourier and Wavelet transforms. Step 2 requires a shrinkage operation for each ℓ^1 term:

$$d^{k+1} = \text{shrink}(u^{k+1} + b^k, \frac{1}{\lambda}) \quad (6)$$

$$w^{k+1} = \text{shrink}(Wu^{k+1} + b_w^k, \frac{1}{\gamma}) \quad (7)$$

Finally, the last two variable updates completes the iteration:

$$b^{k+1} = b^k + (u^{k+1} - d^{k+1}) \quad (8)$$

$$b_w^{k+1} = b_w^k + (Wu^{k+1} - w^{k+1}) \quad (9)$$

Notice that the two shrinkage operations, and the two variable updates are independent of each other and can be computed in parallel.

Step 1 and 2 are embedded in an outer and an inner iterations. The inner iteration is responsible for finding the minimum of Equations 2 and 3, while the outer iteration controls global convergence.

We have designed and implemented an object oriented package in Python in which the user can extend existing classes by providing code for step1 and step 2 for each new ℓ^2 and ℓ^1 term, respectively. In addition to the simple problem 1, we have derived the equations for step 1 and 2 for the following cases:

$$\min_u |\nabla u|_1 + \mu||y - RFu||_2^2 \quad (10)$$

$$\min_u |Wu|_1 + \mu||y - RFu||_2^2 \quad (11)$$

$$\min_u |u|_1 + |Wu|_1 + \mu||y - RFu||_2^2 \quad (12)$$

$$\min_u |\nabla u|_1 + |Wu|_1 + \mu||y - RFu||_2^2 \quad (13)$$

The software can be easily extended to include new ℓ^1 penalizers, and additional convex, differentiable error terms. It is also possible to change or add different sparsity basis operators.

3 Experiments and Results

In order to test the algorithms, we carried out image synthesis experiments with two ALMA continuum data sets of protoplanetary disks. The first one is HLTau, Band 6 [7] and the second one is HD 100546, also Band 6 [8]. Visibilities were gridded with robust parameter -2.0 and 0.5 for HLTau and HD100546, respectively. No apodization was carried out over the data. In both cases, images of 2048×2048 cells, with angular resolution of 0.003 arcsec were reconstructed. HLTau was synthesized using the ℓ^1 norm of the isotropic Total Variation (TV) of the image (Equation 10), whereas HD100546 was reconstructed with the ℓ^1 norm on both wavelet and image domain (Equation 13).

To numerically asses the results, we computed two simple reconstruction performance measures. The Root Mean Square Error (RMSE), and the Peak Signal-to-Noise Ratio (PSNR) of the reconstructed solution u. We use the following version of PSNR:

$$\text{PSNR} = 20 \log_{10}\left(\frac{u_{\max}}{\sqrt{RMSE}}\right) \quad (14)$$

where RMSE is calculated from the residual image.

Resulting images are shown in Figure 1. Images have been zoomed in for easier visualization. The algorithms were run with 20 inner iterations, and a single outer iteration, taking only 37 and 24 seconds for HLTau and HD100546, respectively, on a single intel Core i7 processor.

Table 1 lists the performance measures obtained. It can be seen visually and from the RMSE values that the algorithms are able to supress background noise in both cases. In the case of HLTau, the isotropic TV penalizer has also proved effective in reducing incomplete uv sampling artifacts that show in the dirty image, without reducing image resolution. Even though PSNR values appear to be in acceptable ranges, we cannot advance further conclusions without comparing them to other reconstruction methods.

Table 1. Performance measures

Data	Penalizer	RMSE	PSNR (dB)
HLTau	$\|\nabla u\|_1$	6.18×10^{-7}	49.9
HD100546	$\|u\|_1 + \|Wu\|_1$	4.76×10^{-7}	36.2

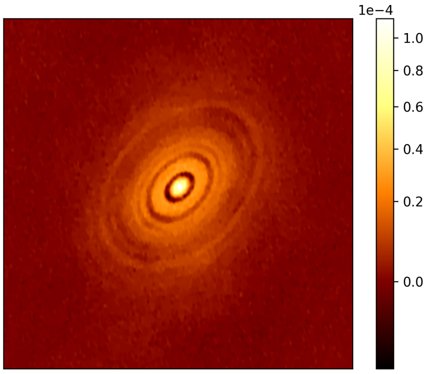

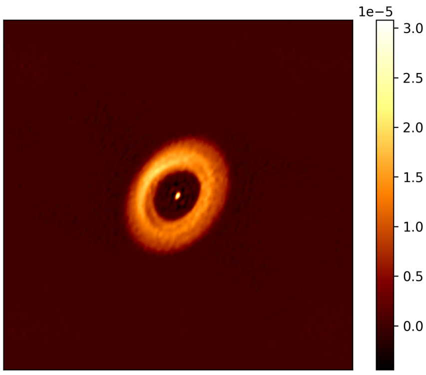

Figure 1. Reconstructed images of (top) HLTau with Equation 10, and (bottom) HD100456 with Equation 13.

4 Conslusions

These preliminary results are very promising and open a new line of research in interferometric imaging. The experiments showed that the SB iteration can produce good quality images on real ALMA data. The object oriented framework together with the SB formulation are suitable for formulating new optimization problems and incorporating them seamlessly into the code. Further work is required to compare this approach to other imaging synthesis methods, in terms of image quality and also in terms of computational footprint.

5 Acknowledgements

This works has been partially supported by FONDECYT 1191934 and by ANID—Millennium Science Initiative Program Center Code NCN2021_080.

References

[1] T. J. Cornwell and K. F. Evans, “A Simple Maximum Entropy Deconvolution Algorithm”, *Astron. Astrophys.* **143**, 1985, pp. 77–83.

[2] M. Cárcamo et al, “Multi-GPU Maximum Entropy Image Synthesis for Radio Astronomy, *Astronomy and Computing*, **22**, 2018, pp. 16-27.

[3] B. Zadwadzki, et al, “Regularized Maximum Likelihood Image Synthesis and Validation for ALMA Continuum Observations of Protoplanetary Disks”, *Publication of the Astro. Soc. of the Pacific, **135**, 064503, 2023*

[4] T. Goldstein and S. Osher, “The Split Bregman for L1-Regularized Problems”, *SIAM J. Imaging Sciences*, **2**, 2, 2009, pp. 323–343.

[5] Y. Wiaux, L. Jacques, G. Puy, A. M. Scaife, and P. Vandergheynst, “Compressed sensing imaging techniques for radio interferometry”, *Monthly Notices of the Royal Astronomical Society*, **395**, 3‘, 2009, pp. 1733–1742.

[6] B. Adcock et al, “Breaking the Coherence Barrier: A New Theory for Compressed Sensing”, *Forum of Mathematics, Sigma*, **5**, e4, 2017.

[7] E. Akiyama, et al, “Planetary System Formation in the Protoplanetary Disk Around HL Tauri”, *The Astrophysical Journal*, **818**:158, 2016.

[8] S. Casassus, S. Pérez, “Kinematic Detections of Protoplanets: A Doppler Flip in the Disk of HD 100546”, *The Astrophysical Journal Letters*, 883:L41 (7pp), 2019.